Journal of Photochemistry and Photobiology A: Chemistry 215 (2010) 76–80

Contents lists available at ScienceDirect

Journal of Photochemistry and Photobiology A: Chemistry

journal homepage: www.elsevier.com/locate/jphotochem

Photocatalytic study of BiOCl for degradation of organic pollutants under UV irradiation

Feng Chen*, Hongqi Liu, Segomotso Bagwasi, Xingxing Shen, Jinlong Zhang

Key Lab for Advanced Materials and Institute of Fine Chemicals, East China University of Science and Technology, 130 Meilong Road, Shanghai 200237, PR China

ARTICLE INFO

Article history:
Received 15 March 2010
Received in revised form 24 June 2010
Accepted 22 July 2010
Available online 30 July 2010

Keywords:
BiOCl
Chlorides
Chlorine radical
Photocatalysis
Photostability

ABSTRACT

BiOCl exhibited high photocatalytic activities for the degradation of rhodamine B, methyl orange and phenol. Surface chloride ions were adverse to the BiOCl photocatalysis and dissociated from BiOCl via reaction with photogenerated holes and electrons under UV irradiation. Conduction band electrons of BiOCl directly reduced either chlorine radical or the azo-bond of MO during the photocatalytic process. Hydroxyl radical was the main oxidative species in the BiOCl photocatalysis, whose generation can be accelerated via enhancing the conduction band electron consumption by MO. After the photocatalytic reaction, the dissolved chloride ion would spontaneously recombine back to the BiOCl photocatalyst, hence qualifies BiOCl as a practical high-activity photocatalyst with long lifetime.

1. Introduction

Semiconductor photocatalysis has attracted increasing attention as a potential environmental technology for wastewater remediation [1–5]. The most utilized photocatalysts are metal oxides such as TiO_2 [1,2], while halides such as AgCl and AgBr have been found to exhibit higher activities than metal oxides for the degradation of dyes [3–5]. The main drawback for the metal halide photocatalyst is their poor photostability, as metal halide bond is possibly cleaved under irradiation [4]. Recently, Huang and Yu reported highly enhanced photostability of silver halides combined with a small amount of Ag^0 [3,5], however, the worry on the lifetime of silver halides still remained, as the photolytic reaction of AgX to Ag^0 and X_2 in aqueous solutions is an irreversible process.

Photocatalysis mechanism of metal oxide semiconductor has been well investigated, in which hydroxyl radical and superoxide radical from the photogenerated hole and electron are confirmed as the main active species responsible for the degradation of organic compounds in aqueous solution [6,7]. However, in the halide/oxyhalide photocatalysts, the valence band is composed of p orbital of halides instead of O_{2p}. Therefore, there is a high possibility that a halide radical instead of •OH radical is the active species responsible for the degradation under UV irradiation. A well-known phenomenon is the photo-decomposition of AgCl, which results in Ag^0 and Cl atom [3]. In addition, the photolysis of other chlorides such as ferric chloride ($[FeCl]^{2+}$) also produce Cl atom, namely, •Cl radical [8]. Thus, undesired organic halides would possibly be produced as the products of Cl radicals attack on organics.

Like halides, oxyhalides are also indirect band-gap semiconductors, which have comparatively slow recombination rate for photogenerated electrons and holes. Consequently, they usually exhibit high activity in photocatalytic applications. As an oxyhalide photocatalyst, BiOCl has a similar valence band (VB) as that of AgCl, which is mainly composed of Cl_{3p} orbital. BiOCl showed a significant photocatalytic reactivity for organic degradation in either gas or aqueous solution [9,10], which is much higher than the commercial P25 TiO_2 photocatalyst. However, if BiOCl photocatalytic reaction generates undesirable organic chlorides and/or BiOCl exhibits poor photostability, BiOCl photocatalysis would not be employed in practical use as an environmental-unfriendly method. Hence, an investigation into the photocatalytic mechanism of BiOCl was carried out in this work. The degradation of methyl orange (MO), rhodamine B (RhB) and phenol were traced. Active oxidative species as well as possible chloride-containing by-products were detected with the fluorescence spectroscopy, while chloride ions were measured with ion chromatography.

2. Experimental

2.1. Preparation of BiOCl photocatalyst

BiOCl photocatalyst was prepared according to the literature procedure [11] except CTAC instead of KCl was adopted as a chloride source [12]. 1.96 g $Bi(NO_3)_3{\cdot}5H_2O$ and 1.31 g cetyltrimethyl

* Corresponding author. Tel.: +86 21 64252062; fax: +86 21 64252062.
E-mail address: fengchen@ecust.edu.cn (F. Chen).

1010-6030/$ – see front matter © 2010 Elsevier B.V. All rights reserved.
doi:10.1016/j.jphotochem.2010.07.026

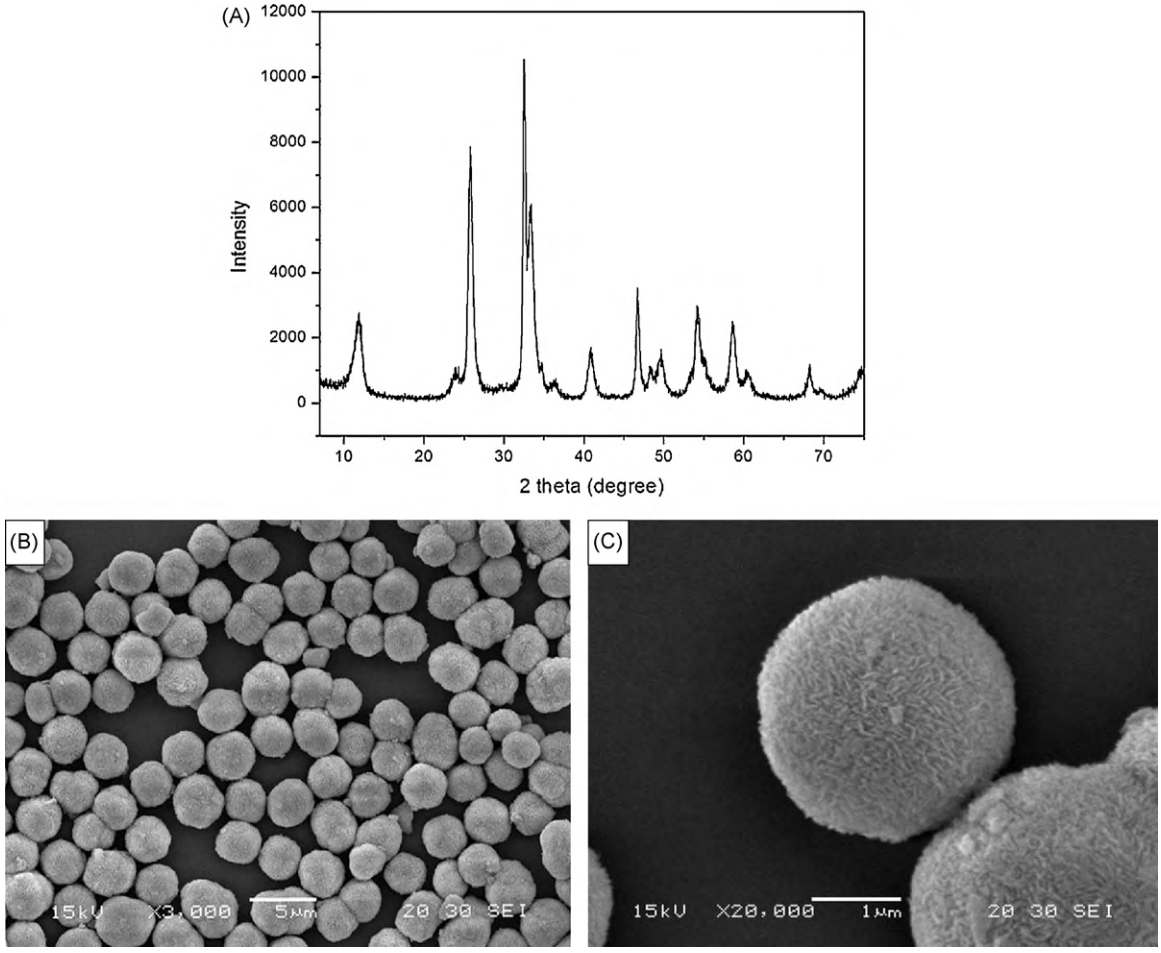

Fig. 1. (A) XRD pattern and (B and C) SEM images of the as-prepared BiOCl.

ammonium chloride (CTAC) were dissolved in 80 mL ethylene glycol (EG), pH of the solution was then adjusted to 1.0 with KOH/EG solution (1.0 M). The resulting solution was then kept at 160 °C for 12 h in a 100 mL Teflon-lined stainless autoclave. In order to avoid the possible interference of organic species, the obtained powder was irradiated with ultraviolet light for 2 h after careful washing. The as-prepared powder was BiOCl microsphere composed of numerous BiOCl nanoplates (Fig. 1, S_{BET} = 8.0 m^2/g).

2.2. Photocatalytic activity measurement

In a typical photocatalytic experiment, aqueous suspension of MO (60 mL, 20 mg/L), RhB (60 mL, 20 mg/L) and 0.06 g photocatalyst powder were placed in a quartz tube with vigorous agitation. The pH value of the aqueous solution was adjusted to 5.00 for MO and 6.86 for RhB with HCl solution. UV irradiation was carried out using a 300 W high-pressure mercury lamp (Yaming Lighting). The distance between the light and the center of quartz tube was 20 cm.

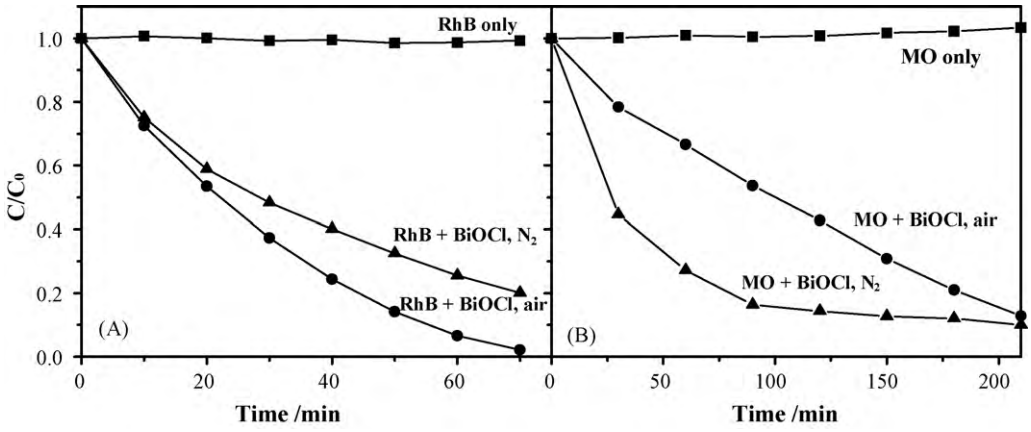

Fig. 2. Degradation of (A) RhB (20 mg/L, pH 6.86) and (B) MO (20 mg/L, pH 5.00) with BiOCl under UV irradiation.

During the reaction, the water-jacketed photochemical reactor was cooled with water-cooling system to maintain the solution at room temperature. Prior to irradiation, the suspensions were stirred in the dark for 0.5 h to allow an adsorption–desorption equilibrium. At irradiation time intervals, 4.0 mL of the suspensions was collected and then centrifuged to remove the photocatalyst powder. A Cary 100 UV–vis spectrometer was used to record the change of concentration of dyes during light irradiation.

2.3. Hydroxyl radical detection

Relative concentration of hydroxyl radical was measured with a fluorescent method. Hydroxyl radicals reacted with 3.0 mM terephthalic acid, and their concentrations were deduced semi-quantitatively from the fluorescent intensity of hydroxyterephthalic acid at 425 nm (excitation wavelength: 312 nm).

2.4. Intermediates detection

Reaction intermediates detection was carried out in the degradation of 1.0 mM phenol. After a given irradiation time, samples of 4.0 mL were withdrawn, and centrifuged to remove the photocatalyst powder. Then the fluorescence spectra of the corresponding intermediates in the supernatant were measured with a Cary Eclipse spectrophotofluorometer under different excitation wavelengths. Chloride ion detection was performed on an ion chromatography (DIONEX, DX 600).

3. Results and discussion

MO and RhB were selected as the target pollutants to trace the photocatalytic activity of BiOCl under the UV irradiation. The dyes were both degraded smoothly under either aerated or deaerated condition as shown in Fig. 2. Most surprisingly, the degradation of MO was even enhanced by N_2 bubbling. Present knowledge on the photocatalytic mechanism shows that the surface redox reactions initiated by photogenerated electrons and holes start the photocatalytic degradation of organics. If the surface chemical reactions of CB electrons are blocked, the VB holes would tend to be consumed by the accumulated electrons via the electron–hole recombination inside the BiOCl nanoparticles; hence, the photocatalytic degradation process would be significantly suppressed. For example, the photocatalytic activity of TiO_2 is nearly lost in the absence of oxygen [13].

The cathode reaction of TiO_2 photocatalysis is usually regarded as the reaction of electron with pre-adsorbed oxygen molecules and thus would be blocked by N_2 bubbling. However, since the degradation rate of MO over BiOCl particles was not reduced by the N_2 bubbling, some other factors should be considered. BiOCl is an indirect band structure material with a band gap of 3.50 eV. The potentials of conduction band (CB) and VB for BiOCl are −1.1 and 2.4 eV, while those for anatase TiO_2 are −0.3 and 2.9 eV [14,15], respectively. As we know, electron transfer depends greatly on the energy difference between the CB and the reduction potential of the acceptor redox couple. The CB electron in the BiOCl has much negative redox potential than that in the TiO_2. Therefore, besides the reaction of electrons with adsorbed oxygen molecules, it is possible that CB electron directly reduce adsorbed organics, which led to the faster degradation of MO under the N_2 bubbling.

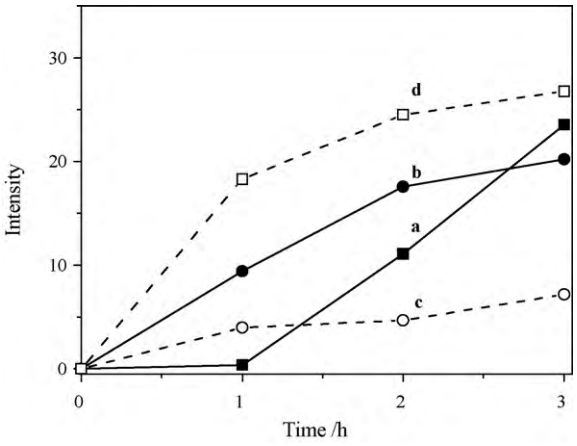

Fig. 3. Fluorescent intensity of terephthalic acid (3.0 mM) aqueous solution at 425 nm with BiOCl under UV irradiation (a) in the absence of MO in air atmosphere, (b) in the presence of MO in air atmosphere, (c) in the absence of MO in N_2 atmosphere and (d) in the presence of MO in N_2 atmosphere.

To further study the photocatalytic mechanism of BiOCl, hydroxyl radicals were measured with a fluorescent method. By reacting with terephthalic acid, hydroxyl radical can be analyzed semi-quantitatively from the fluorescent intensity of hydroxyterephthalic acid at 425 nm [16]. Fig. 3 shows the fluorescent intensity changes vs irradiation time under various conditions. In the absence of MO, the generation of ·OH was obviously decreased by N_2 bubbling. According to the previous literatures in TiO_2 photocatalysis [13], it should be due to the cutting off of the cathode reaction between the CB electron and the oxygen, which favors the charge recombination. However, in the presence of MO, the generation of ·OH was even enhanced with the N_2 bubbling. The generation of ·OH was significantly increased by MO either with or without the N_2 bubbling. It is presumed a direct reduction occurred under the UV irradiation between the CB electron and

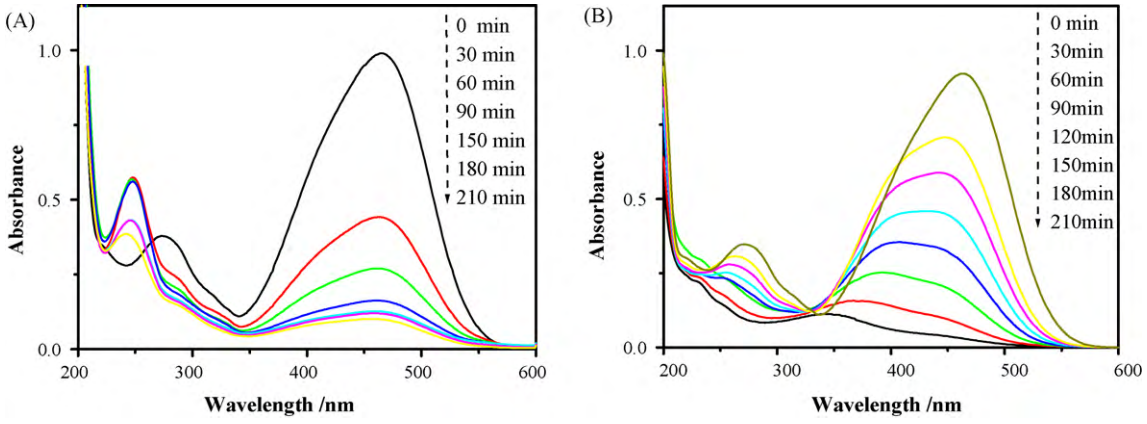

Fig. 4. UV–vis spectra of methyl orange degradation (A) with and (B) without N_2 bubbling.

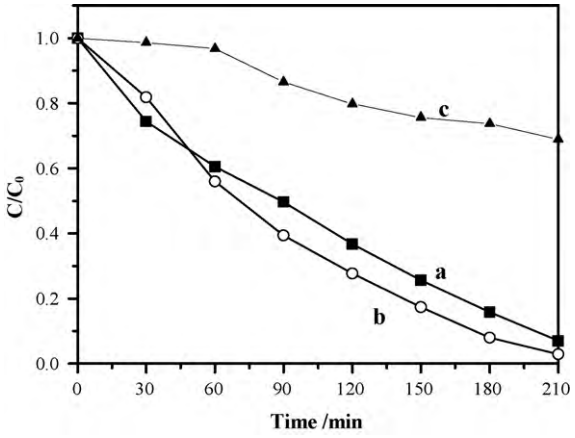

Fig. 5. The photocatalytic degradation of MO with BiOCl under UV irradiation in the (a) absence and (b) presence of 50 mM methanol, and (c) presence of 3.0 mM terephthalic acid.

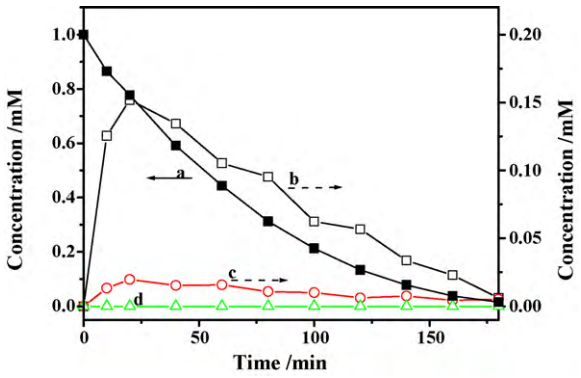

Fig. 6. Concentration variation of (a) phenol and its degradation intermediates, (b) catechol, (c) hydroquinone and (d) 2-chlorophenol/4-chlorophenol.

the adsorbed MO, and consequently promoted the electron–hole separation. From the UV–vis spectra obtained during the MO degradation (Fig. 4), a new UV absorbance peak at 246 nm appeared under N_2 bubbling, and it was not observed in the presence of O_2. Electron reduction of azo dyes has been reported elsewhere [17,18]. The new absorption can be attributed to the electron reduction of azo band, which resulted in the generation of hydrazine derivative [19].

Therefore, in the presence of O_2, the reaction of CB electron with adsorbed oxygen molecules competes with the direct electron reduction of azo-bond, which leads to the relatively slow degradation kinetics of MO. As for the xanthene dye RhB, due to the absence of oxidative groups, a direct electron reduction can hardly take place. Therefore, the degradation of RhB was significantly reduced by N_2 bubbling, which is common observation in TiO_2 photocatalysis.

Several possible primary active oxidative species exists in the BiOCl photocatalytic reaction: •OH radical, hole and •Cl radical. •OH radical seemed to be predominant as a great amount of hydroxyl adducts were detected in the fluorescent spectra. Alcohol was proved to be an effective hole-trapper according to previous study [20]. If holes act as a main oxidative species in a photocatalytic system for the degradation of organics, the addition of alcohol would decrease the degradation kinetics. However, the photocatalytic degradations of MO by BiOCl were not affected by the addition of 50 mM methanol (Fig. 5). Therefore, in this regard, it can be confidently concluded that photogenerated holes were not the main oxidative species in BiOCl photocatalysis in aqueous solution. Photogenerated holes should react with the adsorbed water and surface hydroxyl group to produce hydroxyl radical, which process was however not inhibited with 50 mM of methanol in the presence of 55.5 M water solvent. Chlorine radical (1.359 eV) has lower oxidative potential than that of •OH radical (1.7 eV). It has been reported that •OH radical in aqueous solution would oxidize Cl^- anion to produce •Cl radical, which is adverse to the oxidation of organics [21]. However, one should notice that the potential of valence band of BiOCl is 2.4 eV (although it is also composed of 3p orbital of Cl atom), much more positive than that of •OH radical. The reaction between photogenerated holes from BiOCl photocatalyst with adsorbed water or hydroxyl group is favored to produce •OH radical. As shown in Fig. 5, the degradation of MO by BiOCl greatly decreased in the presence of 3.0 mM terephthalic acid, which acted as a good scavenger for •OH radical.

However, if •Cl radicals were bleached from the BiOCl or the possible reaction between Cl^- anions and photogenerated holes or secondary •OH radicals occurred, the risk of the production of organic chlorides still remains. Hence, the degradation intermediates of phenol were carefully investigated from fluorescent spectra to check for the possible chloride-adducts of phenol.

In general, phenol and phenolic compounds have strong fluorescence under suitable UV excitation, which is highly sensitive and selective [22]. Such characteristics can be used to determine a particular phenolic compound in the aqueous solution. By choosing proper excitation wavelengths for phenol (λ_{ex} = 267 nm, λ_{em} = 296 nm), catechol (λ_{ex} = 286 nm, λ_{em} = 324 nm), hydroquinone (λ_{ex} = 303 nm, λ_{em} = 333 nm), and 2-chlorophenol/4-chlorophenol (λ_{ex} = 232 nm, λ_{em} = 346 nm), phenol and its inter-

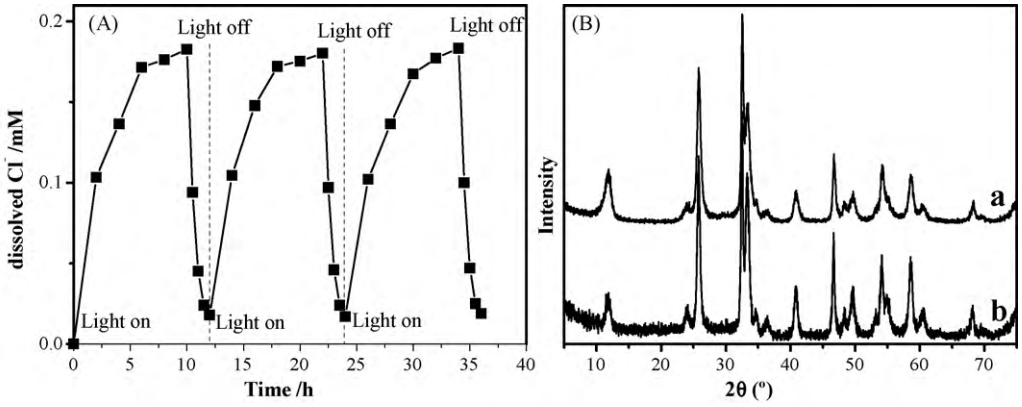

Fig. 7. (A) Concentration change of dissolved Cl^- anion in phenol/BiOCl suspension under UV irradiation and (B) the XRD patterns of BiOCl photocatalyst (a) before and (b) after 15 h UV irradiation.

mediates were independently detected from the reaction solution. Fig. 6 shows the concentration variations of phenol and its degradation intermediates. Hydroxyl adducts of phenol such as catechol and hydroquinone were significantly produced, which confirmed a •OH radical-attack mechanism. Chloride-adducts of phenol were not observed throughout the degradation process of phenol, which partially relieved our worry on the generation of organic chlorides.

The cleavage of chloride anion from the BiOCl occurred under UV irradiation (Fig. 7). The concentration of dissolved chloride anion obeyed first-order kinetics and had a final concentration of 0.216 mM (with a UV light intensity of 1.10 mW/cm^2), which is similar to that ever observed with AgCl. Fortunately, the dissolved chloride anion tends to react with the chloride anion-lack powder $BiOCl_{1-x}(OH)_x$ to form BiOCl, as the pK_{sp} of BiOCl is 30.75 ($[BiO][Cl^-] = 1.8 \times 10^{-31}$ M^2). The concentration of dissolved chloride anion was reduced very fast to a very low level in 90 min. The dissolution and recovery of the chloride anion can be repeated many times by turning on and off the UV lamp (Fig. 7A). It was observed that BiOCl photocatalyst can be used repeatedly for organics degradation without any significant changes on its chemical composition. Although the layered structure of BiOCl was a little bit distorted after long time UV irradiation (15 h, Fig. 7B), the lattice structure inside the [BiO] layer was kept almost unchanged. Because of the application of chlorine disinfectant in the water plant, it is reported that the concentration of Cl^- in the tap water of China is varied from 0.14 to 1.4 mM, e.g., $[Cl^-]$ in the tap water of Shanghai is ca. 1.4 mM. Further, the municipal effluents and the industrial wastewater generally contain a concentration of Cl^- higher than several hundreds mg/L. Therefore, although the recovery of BiOCl was observed to proceed in batch reactor in this work, the application of BiOCl for the flow reactor seems applicable to tap water, the municipal effluents and the industrial wastewater without chloride dissolving. However, as for natural water which has a low $[Cl^-]$ level (0.02 mM to more than 4.0 mM [23–25]), further modification of BiOCl material is need to avoid the Cl^- escaping from the photocatalyst for the potential application in the flow reactor.

A possible reaction pathway for chlorine atom in BiOCl photocatalysis might be related to both photogenerated hole and electron. Surface chloride ions on BiOCl capture the photogenerated holes resulting in the generation of bonded •Cl radical, which lead to the weakening of bond between the chlorine and bismuth atoms. However, •Cl radical tends to react with photogenerated electron even after it separated from the BiOCl. As a result, dissolved Cl^- ions instead of active •Cl radicals were found in the BiOCl photocatalysis. Therefore, a relative chloride anion-lacked surface would be more beneficial for the photocatalytic performance of BiOCl, as the consumption of photogenerated hole by surface chloride ions would be reduced. Fig. 8 shows the degradation of MO with normal BiOCl, surface Cl^- abundant BiOCl and surface Bi^{3+} abundant BiOCl. Surface accumulation of Cl^- and Bi^{3+} was performed in 0.5 M KCl/EG solution and 1.0 mM $Bi(NO_3)_3$/EG solution for 12 h, respectively. The as-prepared samples were washed with EG and water for several times to remove the physical adsorbed ions. Surely, accumulation of Cl^- on the surface of catalyst was harmful to the photocatalytic activity of BiOCl, while accumulation of Bi^{3+} enhanced the photocatalytic degradation of MO.

4. Conclusions

BiOCl exhibited high photocatalytic activities for the degradation of RhB, MO and phenol. BiOCl exhibited strong reduction ability due to the CB potential of −1.1 eV; therefore, a direct reduction of azo-bond was observed in the photodegradation of MO. Hydroxyl radical was the main oxidative species in the BiOCl photocatalysis,

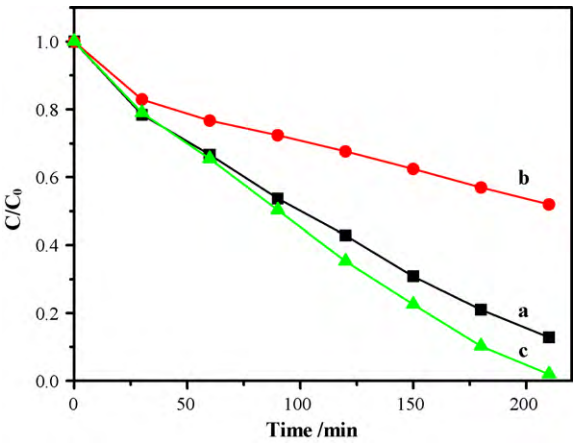

Fig. 8. Degradation of MO (20 mg/L) under UV irradiation with (a) BiOCl, (b) surface Cl^- abundant BiOCl and (c) surface Bi^{3+} abundant BiOCl.

whose generation can be accelerated via enhancing the CB electron consumption by azo dyes such as MO. During the photocatalytic reaction, surface chloride ion captured the photogenerated hole to produce chlorine radical. Immediately, the chlorine radical recombined with the CB electron instead of reacting with organics, which resulted in dissolution of chloride ions. After the photocatalytic reaction, the dissolved chloride ion spontaneously recombines back to the BiOCl photocatalyst, which ensured BiOCl as a practical photocatalyst with long lifetime.

Acknowledgements

This work was supported by the National Science Foundation of China (20777015), National Basic Research Program of China (2010CB732306, 2007CB613301) and the Fundamental Research Funds for the Central Universities.

References

[1] A. Fujishima, T.N. Rao, D.A. Tryk, J. Photochem. Photobiol. C 1 (2000) 1–21.
[2] X.B. Chen, S.S. Mao, Chem. Rev. 107 (2007) 2891–2959.
[3] P. Wang, B.B. Huang, X.Y. Qin, X.Y. Zhang, Y. Dai, J.Y. Wei, M.-H. Whangbo, Angew. Chem. Int. Ed. 47 (2008) 1–4.
[4] Y. Zang, R. Farnood, Appl. Catal. B 79 (2008) 334–340.
[5] J.G. Yu, G.P. Dai, B.B. Huang, J. Phys. Chem. C 113 (2009) 16394–16401.
[6] M.A. Fox, M.T. Dulay, Chem. Rev. 93 (1993) 341–357.
[7] W. Zhao, C. Chen, W.H. Ma, J.C. Zhao, D.X. Wang, H. Hidaka, N. Serpone, Chem. Eur. J. 9 (2003) 3292–3299.
[8] A. Machulek Jr., J.E.F. Moraes, C.V. Giongo, C.A. Silverio, L.C. Friedrich, C.A.O. Nascimento, M.C. Gonzalez, F.H. Quina, Environ. Sci. Technol. 41 (2007) 8459–8463.
[9] N. Kijima, K. Matano, M. Saito, T. Oikawa, T. Konishi, H. Yasuda, T. Sato, Y. Yoshimura, Appl. Catal. A 206 (2001) 237–244.
[10] K.L. Zhang, C.M. Liu, F.Q. Huang, C. Zheng, W.D. Wang, Appl. Catal. B 68 (2006) 125–129.
[11] X. Zhang, Z.H. Ai, F.L. Jia, L.Z. Zhang, J. Phys. Chem. C 112 (2008) 747–753.
[12] H. Deng, J.W. Wang, Q. Peng, X. Wang, Y.D. Li, Chem. Eur. J. 11 (2005) 6519–6524.
[13] H. Gerischer, A. Heller, J. Electrochem. Soc. 139 (1992) 113–118.
[14] S.Y. Chai, Y.J. Kim, M.H. Jung, A.K. Chakraborty, D. Jung, W.I. Lee, J. Catal. 262 (2009) 144–149.
[15] A.L. Linsebigler, G.Q. Lu, J.T. Yates, Chem. Rev. 95 (1995) 735–758.
[16] K.I. Ishibashi, A. Fujishima, T. Watanabe, K. Hashimoto, Electrochem. Commun. 2 (2000) 207–210.
[17] K. Vinodgopal, I. Bedja, S. Hotchandani, P.V. Kamat, Langmuir 10 (1994) 1767–1771.
[18] L.C. Chen, F.R. Tsai, C.M. Huang, J. Photochem. Photobiol. A 170 (2005) 7–14.
[19] G.T. Brown, J.R. Darwent, J. Chem. Soc., Faraday Trans. 1 80 (1984) 1631–1643.
[20] Y. Park, W. Kim, H. Park, T. Tachikawa, T. Majima, W. Choi, Appl. Catal. B 91 (2009) 355–361.
[21] H.Y. Chen, O. Zahraa, M. Bouchy, J. Photochem. Photobiol. A 108 (1997) 37–44.
[22] M.V. Bosco, M. Garrido, M.S. Larrechi, Anal. Chim. Acta 559 (2006) 240–247.
[23] G.L. Han, C.Q. Liu, Chem. Geol. 204 (2004) 1–21.
[24] L.L. Wu, Y. Huh, J.H. Qin, G. Du, S. Van Der Lee, Geochim. Cosmochim. Acta 69 (2005) 5279–5294.
[25] S.Y. Li, Q.F. Zhang, Appl. Geochem. 23 (2008) 3535–3544.